

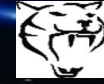
A model for the SED of M87

C. Guennou¹, G.E. Romero^{2,3}, & G.S. Vila²

¹ University of Paris XI, Orsay campus, France

² Instituto Argentino de Radioastronomía, CCT La Plata, CONICET

³ Facultad de Ciencias Astronómicas y Geofísicas, UNLP



Grupo de Astrofísica Relativista y Radioastronomía (GARRA)

1. Abstract

Recent observations with the High Energy Stereoscopic System (HESS) have revealed strong and variable high-energy gamma-ray emission from the radio galaxy M87. The origin of such emission is uncertain, but the rapid variability indicates that it should be produced close to the central engine of the source. In this work, a lepto-hadronic one-zone model is applied to the available multiwavelength data of M87. The different losses for both primary and secondary particles are calculated. Then, the different contributions to the spectral energy distribution through interactions with matter, radiation and magnetic fields are obtained, in good accordance with the observations.

2. Model

In the one-zone approximation (see [1]), the acceleration of particles up to relativistic energies takes place in a compact region through a diffusive shock acceleration mechanism. The location z_{acc} of the one-zone is determined demanding sub-equipartition of the magnetic energy density with respect to the jet internal energy density. The acceleration region extends up to a certain z_{max} , and the one-zone has a thickness of $R_{jet}(z_{max}) = 4 R_g$, where R_{jet} is the radius of the jet. Here we assume the jet injection point is located at a distance $z_0 = 50 R_g$ from the black hole. The jet is supposed to expand as a cone. The radiation processes we have taken into account are: synchrotron radiation, inverse Compton interactions, inelastic proton-proton collisions, and proton-photon interactions. We have also included the radiative contribution of secondary particles (pions, muons and electron-positron pairs). The spectra have been calculated using standard formulae.

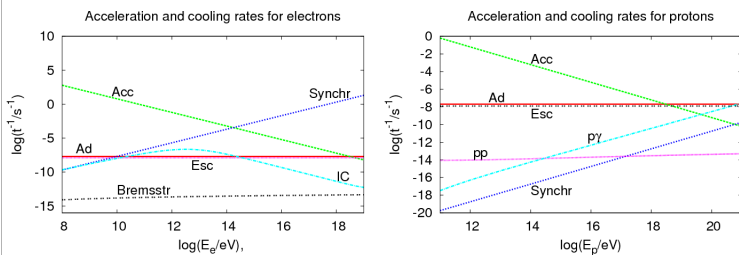


Fig. 1: Acceleration and cooling rates for electrons (left panel) and protons (right panel) in the one-zone. « Ad » and « Esc » denote the adiabatic cooling rate and the escape rate, respectively.

3. Results

Figure 1 shows the acceleration and cooling rates for protons and electrons. The maximum energy for protons and electrons can be estimated by balance the acceleration rate and the cooling rates. The maximum energies are $E_{max} \sim 3 \times 10^{18}$ eV and $E_{max} \sim 1.5 \times 10^{14}$ eV, for protons and electrons, respectively. For the electrons the main channel of energy loss is synchrotron radiation, whereas adiabatic losses is the most relevant channel for the protons. Figure 2 shows the SED obtained. The three main contributions to the luminosity are electron synchrotron radiation and IC scattering peaking at $\sim 10^{40}$ erg s^{-1} , and proton-photon interaction peaking at $\sim 10^{39}$ erg s^{-1} . All radiation emitted by secondary particles is negligible: synchrotron radiation peaks at only $\sim 10^{37}$ erg s^{-1} and IC scattering at $\sim 10^{35}$ erg s^{-1} . With the set of parameter given in Table 1, the data is well fitted. We have also calculated internal absorption effects using the attenuation factor $\exp(-\zeta)$ due to photon-photon annihilation. This process can be important in some models and TeV gamma-rays can be absorbed. However in our case, the spectral energy distribution is not affected, The radiation is completely suppressed only above 10^8 TeV, what is of no observable consequence.

Parameter	[units]	Value
L_{jet}	Jet luminosity [erg s^{-1}]	10^{44}
q_{jet}	Jet content of relativistic particles	0.1
a	Hadron-to-lepton energy ratio	50
Γ_{jet}	Jet bulk Lorentz Factor	4.5
θ	Jet viewing angle	15°
η	Acceleration efficiency	0.1
ϕ	Jet half-opening angle	5°
z_0	Jet launching point [cm]	$50 R_g \sim 2 \times 10^{16}$ cm
α	Particle injection spectral index	2.2
E^{min}	Minimum particle energy	$100 mc^2$
B_0	Magnetic field at the base of the jet [G]	~ 84 G
z_{acc}	Extent of the acceleration region	$\sim 45 z_0$
v_{jet}	Jet bulk velocity [cm s^{-1}]	c
m	Magnetic field decay index	2
M_*	Black hole mass	$3 \times 10^9 M_\odot$
g	Subequipartition parameter	0.6



Table 1. Parameters used to generate the SED shown in Figure 2.

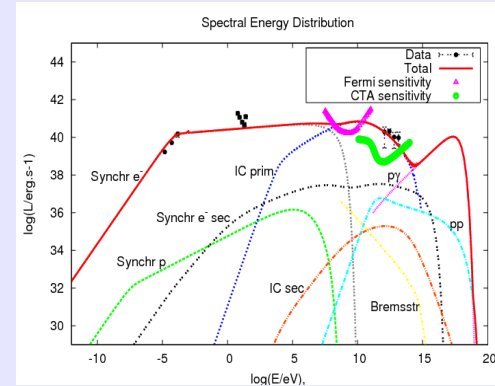
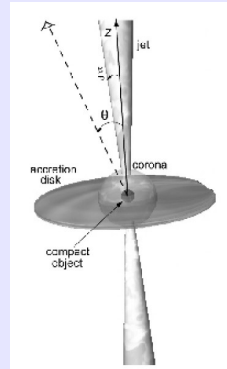


Fig. 2: Left: schematic view of the M87 nucleus and jets (see [2]). Right: spectral energy distribution obtained for the values of the parameters showed in Table 1. The sensitivity of the Cherenkov Telescope Array (CTA) and the Fermi Gamma-Ray Space Telescope are also shown. The data were taken with the X-ray satellite Chandra (see [3]).

4. Conclusion and perspectives

This type of model explain the observed emission mainly with leptonic contributions. The hadronic contribution becomes dominant only at very high energies, between 10^{14} and 10^{19} eV. For such energies M87 may be an important source of neutrinos, through pion and muon decays. The number of muon neutrinos that might be observed should be similar to the number of photons. The future European neutrino detector KM3NET, expected to operate around 2015, might detect this emission. The next step on the modelling of the M87 inner jet emission will consist in the introduction of a mechanism capable of explaining the observed variability. In addition, convection in the inner jet will be considered.

References

- [1] Khangulyan, D., Hnatic, S., Aharonian, F.A., & Bogovalov, S., 2007, MNRAS, 380, 320
- [2] Reynoso M.M. & Romero G.E., 2009, A&A, 493, 1
- [3] Perlmutter, E.S., & Wilson, A.S. 2005, ApJ, 627, 140

Acknowledgements Thanks to the conicet, the IAR and the University of Paris XI for supporting this work. This research was supported by ANPCyT through grant PICT-2007-00848 BID 1728/OC-AR.